

Cytoplasmic Function of Mutant Promyelocytic Leukemia (PML) and PML-Retinoic Acid Receptor- α *[§]

Received for publication, January 17, 2006 Published, JBC Papers in Press, March 15, 2006, DOI 10.1074/jbc.M600457200

Cristian Bellodi^{†§}, Karin Kindle[¶], Francesca Bernassola^{||}, David Dinsdale[‡], Andrea Cossarizza[§], Gerry Melino[‡], David Heery[¶], and Paolo Salomoni^{‡1}

From the [†]Medical Research Council Toxicology Unit, Leicester LE1 9HN, United Kingdom, [¶]School of Pharmacy, University of Nottingham, Nottingham NG7 2RD, United Kingdom, ^{||}IDI-IRCCS Biochemistry Laboratory, Department of Experimental Medicine, University of Rome Tor Vergata, Rome 00133, Italy, and [§]Department of Biomedical Sciences, University of Modena and Reggio Emilia, Modena 41100, Italy

The promyelocytic leukemia (PML) tumor suppressor of acute promyelocytic leukemia (APL) regulates major apoptotic and growth-suppressive pathways. In APL, PML is involved in a chromosomal translocation generating the PML-retinoic acid receptor- α (RAR α) fusion protein. Two missense mutations in the remaining PML alleles have been identified, which give rise to a truncated cytoplasmic PML protein (Mut PML). APL patients carrying these mutations display resistance to retinoic acid (RA) and very poor prognosis. Here we show that Mut PML associates with the cytoplasmic regions we refer to as PML-cytoplasmic bodies (PML-CBs). Mut PML interacts with PML-RAR α in PML-CB and potentiates PML-RAR α -mediated inhibition of RA-dependent transcription. Remarkably, Mut PML stabilizes PML-RAR α and inhibits differentiation induced by pharmacological doses of RA. A mutant form of PML-RAR α that accumulates in the cytoplasm inhibits RA-dependent transcription and differentiation, thus suggesting that cytoplasmic localization of PML-RAR α may contribute to transformation. Finally, we show that the *bcr3* PML-RAR α form is predominantly cytoplasmic and accumulates in PML-CBs. Taken together, these findings reveal novel insights into the molecular mechanisms contributing to APL.

The promyelocytic leukemia (*Pml*) gene encodes a tumor suppressor involved in the t(15;17) chromosomal translocation associated with acute promyelocytic leukemia (APL),² and which produces the fusion protein PML-RAR α (1). Two major isoforms are generated, depending on the location of the *PML* breakpoint, named *bcr1* (long) and *bcr3* (short) (2, 3). PML-RAR α is able to act as a dominant-negative retinoic acid receptor, thus inhibiting the response to RA and blocking RA-induced differentiation (4). This function is mainly exerted through changes at the chromatin level through the recruitment of histone deacetylases and methyltransferases (5–7). However, it is presently unclear whether other mechanisms are involved. Treatment with pharmacological doses of all-*trans*-retinoic acid (ATRA) causes the degra-

tion of the fusion protein and the maturation of the leukemic cells, thus resulting in clinical remission in patients (8). However, 20–30% of patients are insensitive to such treatment and suffer relapse (8). Treatment regimens of such patients include the use of arsenic trioxide, which has a high efficacy (9, 10). On the other hand, PML-RAR α inhibits PML tumor-suppressive functions thus lending the leukemic cells a growth and survival advantage (1). Because the effects of PML-RAR α on PML are dose-dependent (1), the product of the remaining *PML* allele may oppose PML-RAR α -mediated leukemogenesis. Indeed, progressive reduction of the *PML* gene dosage in a murine APL model results in increased incidence and decreased latency of the disease (11). PML is a member of the Ring-B-box-coiled coil (alternatively named tripartite motif, TRIM) family and exists as multiple splicing variants (12). PML nuclear splice variants localize to a subnuclear structure known as the PML-nuclear body (PML-NB), which has been implicated in transcriptional regulation and is disrupted in APL (1). Nuclear PML is essential for the proper formation and stability of these subnuclear structures (1). Several nuclear proteins localize to the PML-NB, such as p53, the p53 acetyltransferase cAMP-response element-binding protein-binding protein (CBP), the cell death regulator Daxx, and Sp100 (1). By contrast, cytoplasmic isoforms are less characterized. One specific cytoplasmic isoform has been associated with transforming growth factor- β signaling (13). Remarkably, a recent study conducted on a cohort of 17 RA-resistant APL cases identified two *Pml* mismatch mutations in the remaining allele, which are associated with very aggressive disease (14). Both mutations (1272delAG and IVS3–1G-A) generate a premature stop codon upstream of the nuclear localization signal. Thus, the resulting truncated proteins accumulate in the cytoplasm (14). Furthermore, another study identified a murine plasmacytoma cell line harboring a *PML* mutation (*mut ex3*), which also leads to a premature stop codon at the end of exon three, cytoplasmic localization and dominant-negative properties (15). PML-RAR α itself undergoes alternative splicing to produce truncated proteins that are predicted to localize in the cytoplasm (16, 17). Localization of PML-RAR α in the cytoplasm has been reported to cause an endoplasmic reticulum stress response and the ubiquitination of N-Cor (18). Moreover, the proteolytic cleavage of PML-RAR α by elastase results in cytoplasmic accumulation of the PML portion of the fusion protein and is probably required for disease progression (19). Thus, accumulating evidence suggests that both PML and PML-RAR α might have a functional role in the cytoplasm.

Although APL-associated PML mutations have been shown to cause PML relocation to the cytoplasm (14), the evidence that PML delocalization has an impact on the sensitivity to maturation signals such as RA was lacking. Here we show that mutant PML potentiates PML-RAR α -mediated block of differentiation and inhibition of retinoic acid-dependent transcription. Moreover, PML mutants form cytoplasmic bod-

* This work was supported by the Medical Research Council. The costs of publication of this article were defrayed in part by the payment of page charges. This article must therefore be hereby marked "advertisement" in accordance with 18 U.S.C. Section 1734 solely to indicate this fact.

§ The on-line version of this article (available at <http://www.jbc.org>) contains supplemental Fig. 1.

¹ To whom correspondence should be addressed. Tel.: 44-116-2525568; Fax: 44-116-2525616; E-mail: ps90@le.ac.uk.

² The abbreviations used are: APL, acute promyelocytic leukemia; PML, promyelocytic leukemia; RAR, retinoic acid receptor; CB, cytoplasmic body; ATRA, all-*trans*-retinoic acid; nls, nuclear localization signal; WT, wild type; DAPI, 4,6-diamidino-2-phenylindole; CBP, cAMP-response element-binding protein-binding protein; PBS, phosphate-buffered saline; HA, hemagglutinin; Mut, mutant; PML-NB, PML-nuclear body; VD3, vitamin D₃; PR, PML-RAR α .

Mut PML and PML-RAR α Have Cytoplasmic Functions

ies (PML-CB), where selective PML-NB components accumulate. PML-RAR α itself accumulates in PML-CB and colocalizes with Mut PML. Finally, we found that a PML-RAR α mutant that accumulates in the cytoplasm retains the ability to inhibit RA-dependent transcription and differentiation.

MATERIALS AND METHODS

Cell Culture—Primary fibroblasts and established cell lines were cultured in Dulbecco's modified Eagle's medium supplemented with 20 or 10% fetal bovine serum, 100 units/ml penicillin, 100 mg/ml streptomycin, 4.5 mg/ml glucose, and L-glutamine. Hematopoietic cell lines HL60, NB4, RA-resistant NB4 (336 and 006, a kind gift of Carlo Gambacorti, Istituto Tumori, Milan, Italy), and U937 were cultured in RPMI 1640 supplemented with 10% fetal bovine serum and 2 mM GlutaMAXTM. All reagents were purchased from Invitrogen.

Cloning and Plasmids Generation—PML mutants (14) as well as PML-RAR α *bcr3* were generated by using PCR-based strategies, tagged at the amino terminus with HA or Myc epitope, and then subcloned into pcDNA3.0 (Invitrogen) and pBABE PURO (20). PML-RAR α *bcr1* (17) was cut from PINCO-PML-RAR α (a kind gift of Dr. Saverio Minucci) and subcloned into pSG5, pcDNA3.0, and pBABE PURO. When not specified, the PML-RAR α form used in this study is *bcr1*. QuikChange[®] site-directed mutagenesis kit was used according to the manufacturer's instructions to delete PML or both PML and RAR nuclear localization signals (nls) of PML-RAR α to generate pcDNA-PML-RAR α - Δ NLS1 and - Δ NLS2, respectively (Δ 1PR and Δ 2PR). PML-RAR α Δ 2 mutant that lacks the capability to bind RXR α has been described elsewhere (21) and was generated using standard PCR-based strategy. Finally, RXR α cDNA was amplified using RNA prepared from human primary fibroblasts (BJ) and subcloned into pcDNA 3.0.

Subcellular Fractionation—For each cell type, subcellular fractionation was performed as described previously (22). Cells were harvested, washed twice in ice-cold PBS, and homogenized using a loose-fitting Dounce homogenizer in ice-cold hypotonic buffer (10 mM Hepes, 10 mM MgCl₂, 1 mM EDTA in the presence of a complete protease/inhibitor mixture). Alternatively, hematopoietic NB4 cells were homogenized using a tight-fitting Dounce homogenizer in ice-cold hypotonic buffer with added 0.25 M sucrose. After that, the homogenate was centrifuged at 1000 \times *g* for 10 min at 4 °C to obtain pellet (P1) and supernatant (S1) consisting of nuclei and whole cytoplasmic extracts, respectively. Pellet P1 was lysed in ice-cold hypertonic buffer (150 mM NaCl, 10 mM Hepes, 10 mM MgCl₂, 1 mM EDTA supplemented with a complete protease/inhibitor mixture), whereas S1 was further centrifuged at 100,000 \times *g* for 1 h at 4 °C to obtain pellet (P100) and supernatant (S100) which represent, respectively, the insoluble (membranes enriched) and soluble cytosolic fractions. Aliquots of each fraction as well as whole cellular lysates were analyzed by SDS-PAGE, transferred onto a nitrocellulose membrane, and probed with relevant antibodies.

Immunoprecipitation—Cells were lysed in immunoprecipitation (IP) buffer (50 mM Tris-Cl, pH 7.6, 150 mM NaCl, 2 mM Na₂VO₃, 2.5 mM NaF, and 0.5% Triton X-100 in the presence of a complete protease/inhibitor mixture). 500 μ g of lysates was subjected to immunoprecipitation using Sepharose beads coated with relevant antibodies for 3 h at 4 °C. Immunocomplexes were washed five times with 500 μ l of IP buffer, resuspended in SDS sample buffer, and then subjected to Western blot analysis.

Western Blots—Western blot analysis was performed as described previously (23). In particular, the effect of Mut PML on PML-RAR α protein levels was assayed upon treatments with ATRA or arsenic tri-

oxide (As₂O₃) in COS1 cells. Briefly, 2.5 \times 10⁵ cells were seeded in a 6-well plate for 12 h before transfection. Transfections were carried out using Lipofectamine 2000 (Invitrogen) according to the manufacturer's instructions. The following expression vectors were transfected: 1600 ng of pcDNA-HAPML-RAR α together with 400 to 200 ng of pcDNA-mycMut PML or empty vector. Eight hours later cells were washed twice with PBS and cultured in the presence or absence of 0.1 μ M ATRA (Sigma) or 1 μ M arsenic trioxide (Sigma). Finally, cells were harvested 12 and 24 h after treatments, and PML-RAR α protein levels were analyzed by Western blot.

Antibodies—Antibodies employed in this study are as follows: rabbit anti-human PML (Chemicon), mouse anti-human PML PG-M3 (Santa Cruz Biotechnology), anti-HA (Sigma), anti-Myc tag (Cell Signaling), anti-EEA1 (BD Biosciences), anti-FLAG (Sigma), anti-RAR α (C20; Santa Cruz Biotechnology), anti-RXR α (Santa Cruz Biotechnology), anti-DAXX human (Upstate Biotechnology, Inc.), anti-Sp100 (a kind gift of Thomas Hofmann) (24), anti-CBP (A22; Santa Cruz Biotechnology), and anti-CD11b fluorescein isothiocyanate-conjugated (Caltag Laboratories). Fluorescein isothiocyanate- and phycoerythrin-conjugated secondary antibodies were purchased from Molecular Probes (Invitrogen), and hypoxanthine-guanine phosphoribosyltransferase-linked secondary antibodies were purchased from Amersham Biosciences.

Immunofluorescence—Immunofluorescence and confocal microscopy was performed as previously described (25).

Electron Microscopy and Immunogold Cytochemistry—Adherent cells were processed and embedded in epoxy resin. Duplicate pellets were fixed with 4% formaldehyde (freshly made up from paraformaldehyde) or a mixture of 4% formaldehyde and 0.1% glutaraldehyde in PBS, pH 7.4, for 1 h at room temperature and rinsed in PBS. A subset of these pellets was post-fixed in a mixture of osmium tetroxide (0.05%) and potassium ferrocyanide (0.05%). All were embedded in LR-White resin (Agar Scientific, Stansted, UK) and labeled with immunogold (British Biocell International, Cardiff, UK) (26). Ultra-thin sections were examined unstained or after staining with lead citrate and/or uranyl acetate. Control incubations involved the replacement of primary antibody with an equivalent concentration of the appropriate immunoglobulin.

Nucleofection—U937 cells were transfected using the Amaxa Nucleofector system (Amaxa GmbH) according to the manufacturer's instructions (protocol V-01).

Transcriptional Assays—Cells (COS1) were seeded 24 h prior transfection in 12-well plates and cultured in Dulbecco's modified Eagle's medium (Invitrogen) supplemented with 10% fetal bovine serum (Sigma), penicillin/streptomycin, and GlutaMAX (Invitrogen). Transfection was carried out by using a calcium phosphate transfection kit (Invitrogen) according to the manufacturer's instructions. For RA-dependent transcription, the following expression vectors were used (100 ng unless otherwise stated): pCH110, 300 ng of pRep₄-RARE-Luc and pcDNA-PML-RAR α alone or in combination with 100 ng of pcDNA-HAMut PML. Fresh medium containing 10⁻⁷ M ligand (ATRA) was added 24 h post-transfection, and cells were incubated for 12 h. Finally, cells were harvested, and 5 μ l of extracts were assayed by using dual light system kit (Applied Biosystem) for luciferase activity according to the manufacturer's instructions. Transcriptional activity of PML-RAR α Δ NLS-1 and -2 mutants was assayed as above. Cells were cultured in Dulbecco's modified Eagle's medium containing 10% fetal bovine serum and transfected with 1 μ g each of pcDNA-PML-RAR α , pcDNA-PR Δ NLS-1, and -2. Effects of PML-RAR μ Δ 2 on dihydroxyvitamin D₃-dependent transcription were investigated in transiently transfected COS1 cells. Briefly, cells were transfected with 300 ng of vitamin D₃ luciferase reporter (consisting of four DR3-type vitamin D₃-responsive elements inserted upstream of the tk-luciferase) (kind gift of Professor Carsten

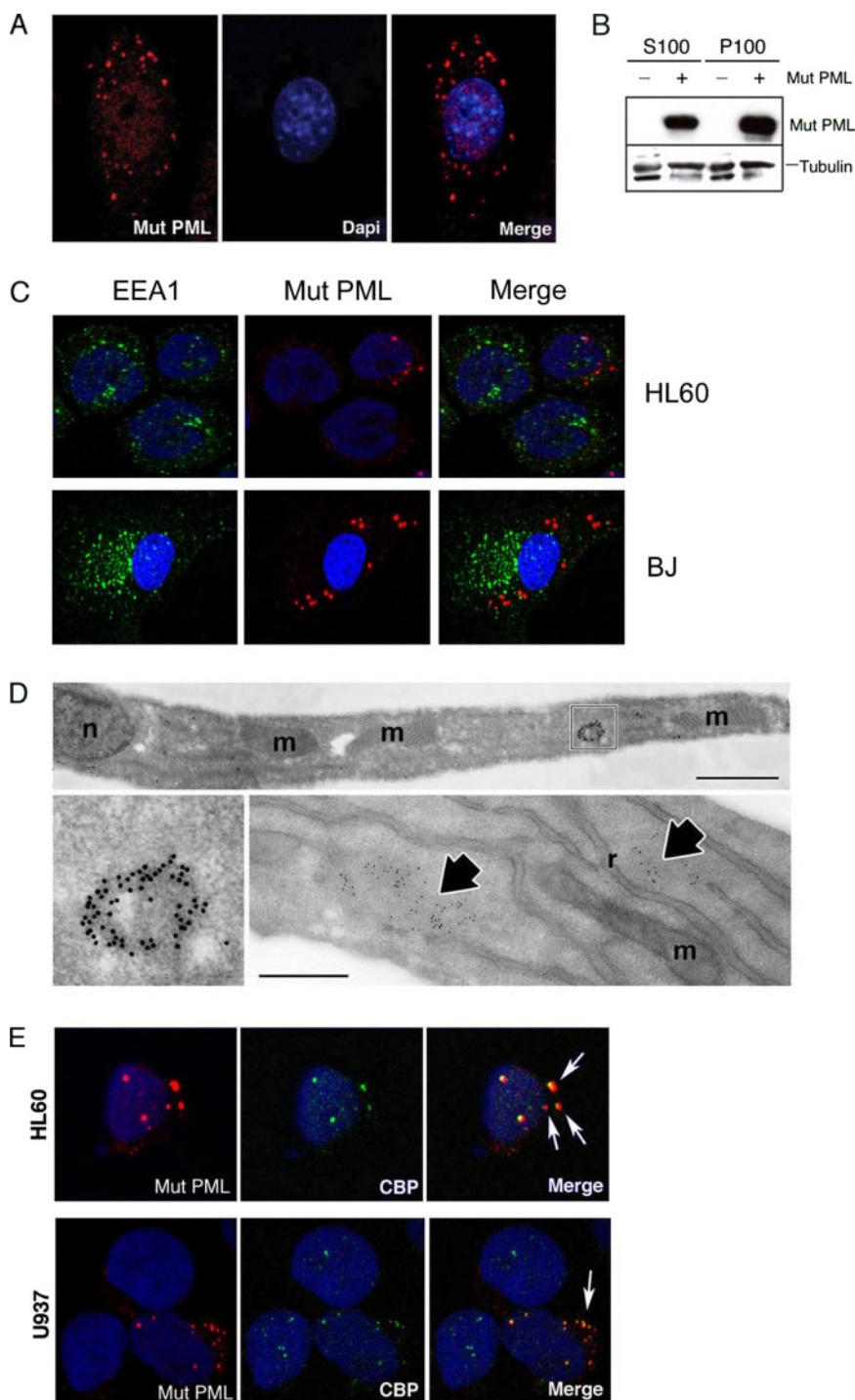


FIGURE 1. Mutant PML forms PML-CB. *A*, mutant PML (Mut PML) forms cytoplasmic bodies. Infected BJ cells were stained using an anti-HA antibody. Nuclei were visualized using DAPI. *B*, Mut PML accumulates in both the soluble and insoluble fraction of the cytoplasm. The pellet P100 and supernatant S100 fractions from Mut PML-transfected fibroblasts were stained with an anti-HA antibody. Tubulin was detected as loading control. *C*, Mut PML does not associate with endosomes. Mut PML-infected cells were fixed and subsequently stained with anti-HA and EEA1 antibodies, and nuclei were detected using DAPI. Slides were analyzed by confocal microscopy. *D*, Mut PML forms doughnut-shaped PML-CB. Immunogold (10 nm) labeling of PML in a PML-CB within the cytoplasm of a MUT PML-transduced cell (*top*; bar = 1 μ m). Detail of a PML-CB indicated above (*bottom left*). Immunogold (5 nm) labeling of HA-tagged Mut PML in the cytoplasm (*bottom right*; bar = 500 nm). *m* indicates mitochondria; *r* indicates endoplasmic reticulum; *n* indicates nucleus. *E*, CBP is recruited to the PML-CB in Mut PML-expressing U937 and HL60 cells. Control and Mut PML-expressing cells were stained anti-HA (red) and anti-CBP antibodies (green; left panel).

Carlberg), 600 ng of PML-RAR α (*bcr-1*), PML-RAR α Δ 2, or pcDNA3.0 vectors along with 100 ng of pCH110. Cells were cultured for 12 h in presence or absence of 10^{-6} M of dihydroxyvitamin D₃ (Calbiochem) and subsequently assayed for luciferase and β -galactosidase activities.

Retroviral Infection—Retroviral infection was performed as described previously (23). For hematopoietic cells, spinoculation was performed by spinning viral supernatants on top of target cells at 2500 rpm for 1 h and 30 min.

Differentiation Analysis—NB4 and U937 cells were infected as described previously (23) using empty and Mut PML or PML-RAR α Δ 2 retroviral constructs, respectively. Infection was carried out using spinoculation. Cells were selected with puromycin and used either as clones or

mixed populations. Differentiation was induced as reported (27) culturing cells with 10^{-7} or 10^{-6} M ATRA. After 4 days, differentiation was assayed by flow cytometry analysis of differentiation surface marker CD11b (Caltag Laboratories). In addition, differentiation was evaluated by morphological analysis of U937 cells following hematoxylin-eosin staining.

RESULTS

Mutant PML Proteins Form Cytoplasmic Bodies—APL-associated PML mutations (1272delAG and IVS3-1G-A) lead to the generation of truncated PML proteins (Mut PML 1 and 2) that lack the nuclear localization signal and accumulate in the cytoplasm (14). We analyzed whether Mut PML 1- and 2-transduced cells displayed alterations in cell

Mut PML and PML-RAR α Have Cytoplasmic Functions

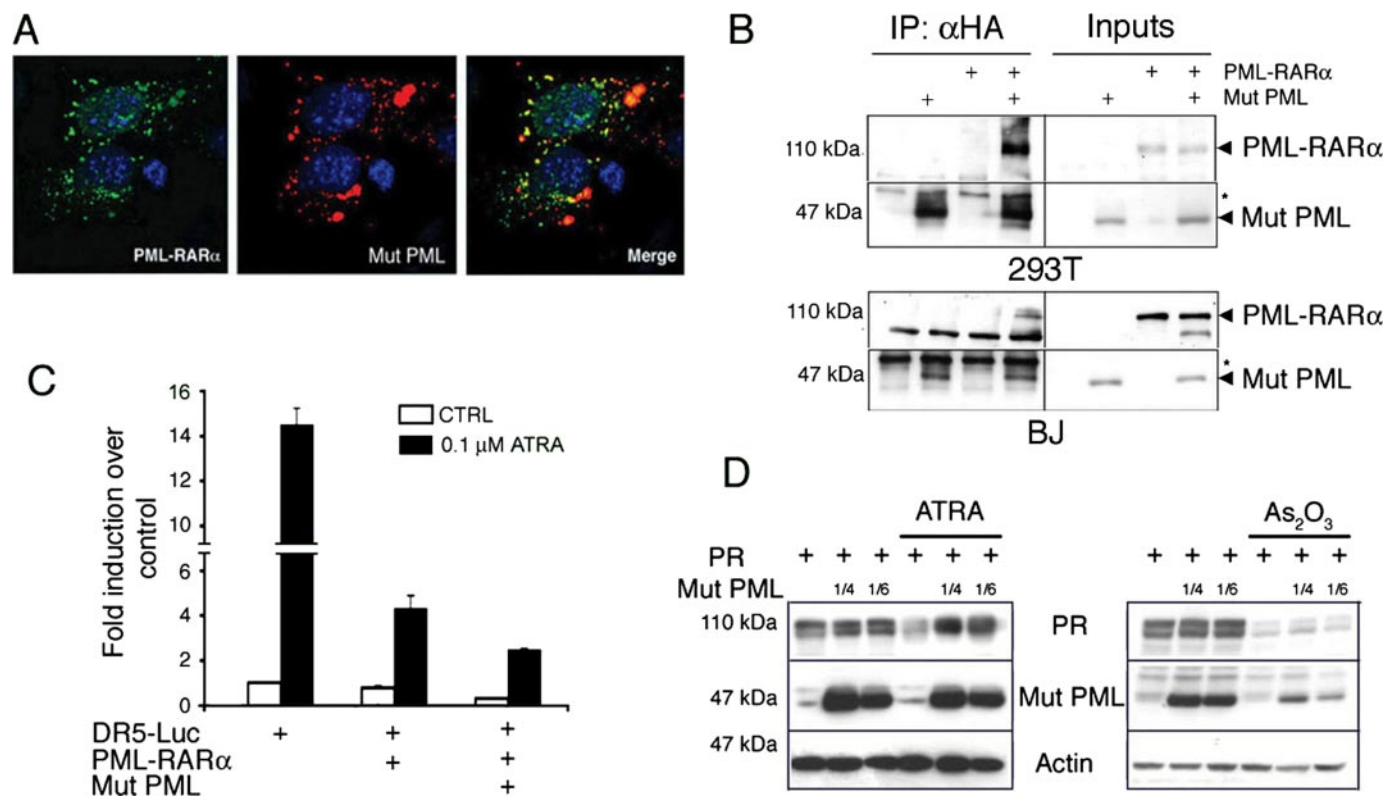


FIGURE 2. Mut PML potentiates PML-RAR α repressive function upon RA. *A*, PML-RAR α colocalizes with Mut PML in PML-CB. PML-RAR α - and HA-Mut PML-infected cells were stained with antibodies anti-RAR α (green) and anti-HA (red). DAPI was used to counterstain nuclei. *B*, PML-RAR α and Mut PML interact in cells. Interaction between PML-RAR α and HA-Mut PML was assayed in transfected 293T and BJ cells by coimmunoprecipitation experiments. Anti-HA immunoprecipitates (IP) were probed with anti-RAR α and anti-HA antibodies. *C*, Mut PML potentiates PML-RAR α -mediated transcriptional inhibition. COS1 cells were transfected with different combinations of DR5-luciferase reporter (*DR5-Luc*), PML-RAR α , and Mut PML in the presence or absence of 0.1 μ M RA. *D*, Mut PML inhibits RA-mediated PML-RAR α down-regulation. COS1 cells were transfected with Myc-Mut PML and HA-PML-RAR α vectors and treated with 1 μ M RA or 1 μ M As₂O₃. Lysates were probed with anti-Myc, anti-HA, and anti-actin antibodies.

death and proliferation at steady state and failed to detect any substantial changes, thus demonstrating that, unlike nuclear PML, these mutants are not growth-suppressive or pro-apoptotic *per se* (not shown). Then we studied the localization pattern of Mut PML 1 and 2 in transfected fibroblasts. Both proteins displayed an identical localization pattern and accumulated to discrete foci, which we refer to as PML cytoplasmic bodies (PML-CB; Fig. 1*A* and supplemental Fig. 1*A*). As both proteins displayed the same localization pattern, we decided to focus on Mut PML 1 (Mut PML) for all our subsequent analyses. In subcellular fractionation experiments, a portion of Mut PML accumulated in the P100 fraction, suggesting that the Mut PML-positive foci associate with the insoluble part of the cytoplasm, which contains intracellular membranes (Fig. 1*B*). As a recent study indicated that cytoplasmic PML isoforms are associated with early endosomes (13), we attempted to verify whether Mut PML colocalizes with the early endosomal marker EEA1 but failed to reveal a colocalization with these organelles (Fig. 1*C*). We also analyzed the distribution of Mut PML in relation to mitochondria, lysosomes, and endoplasmic reticulum using the appropriate markers but again failed to prove significant colocalization (not shown). To better assess the structural features of PML-CB, we performed electron microscopy studies using antibodies directed against PML or the HA tag. Mut PML formed doughnut-shaped structures as shown by EM, which are reminiscent of the PML-NB (Fig. 1*D*), and did not colocalize with intracellular organelles such as mitochondria and endoplasmic reticulum (*m* and *r*; Fig. 1*D*, bottom right). The PML-NB components Daxx and Sp100 did not associate with PML-CB upon coexpression of Mut PML in fibroblasts and hematopoietic cells (supplemental Fig. 1*B* and not shown). In contrast, although CBP was exclu-

sively nuclear in the majority of control cells examined, coexpression of Mut PML caused CBP accumulation in PML-CB in both hematopoietic cells and fibroblasts (Fig. 1*E* and supplemental Fig. 1, *C* and *D*). Furthermore, the number of CBP-containing PML-NBs was substantially reduced in Mut PML-expressing cells (supplemental Fig. 1*C*). Finally, CBP staining was competed out using a specific peptide (supplemental Fig. 1*D*).

Mut PML Potentiates PML-RAR α Function—PML-RAR α acts as a strong inhibitor of the RA receptor complex, thus causing a block of RA-dependent transcription and differentiation (4). We reasoned that Mut PML could affect PML-RAR α -mediated inhibition of RA-dependent processes in leukemic cells. As both Mut PML and PML-RAR α contain the Ring-B-box-coiled coil motif, they can potentially interact and form heterodimers. To test this, we coexpressed Mut PML and PML-RAR α and found that they partially colocalized in cytoplasmic bodies (Fig. 2*A*). Furthermore, we were able to coimmunoprecipitate PML-RAR α and Mut PML in transfected 293T cells and fibroblasts (Fig. 2*B*). Remarkably, we found that expression of Mut PML potentiated the inhibition of ATRA-dependent transcription exerted by PML-RAR α (Fig. 2*C*). To uncover the potential mechanisms underlying the Mut PML-mediated effect on PML-RAR α , we analyzed the effect of Mut PML expression on PML-RAR α down-regulation upon ATRA treatment. Expression of Mut PML resulted in impaired PML-RAR α down-modulation in the presence of different concentrations of ATRA (0.1 and 1 μ M; Fig. 2*D* and not shown). Instead, Mut PML did not affect arsenic trioxide (As₂O₃)-mediated down-regulation of PML-RAR α (Fig. 2*D*). However, As₂O₃ caused reduction of Mut PML protein levels as well, thus explaining the lack of protection (Fig. 2*D*). To determine

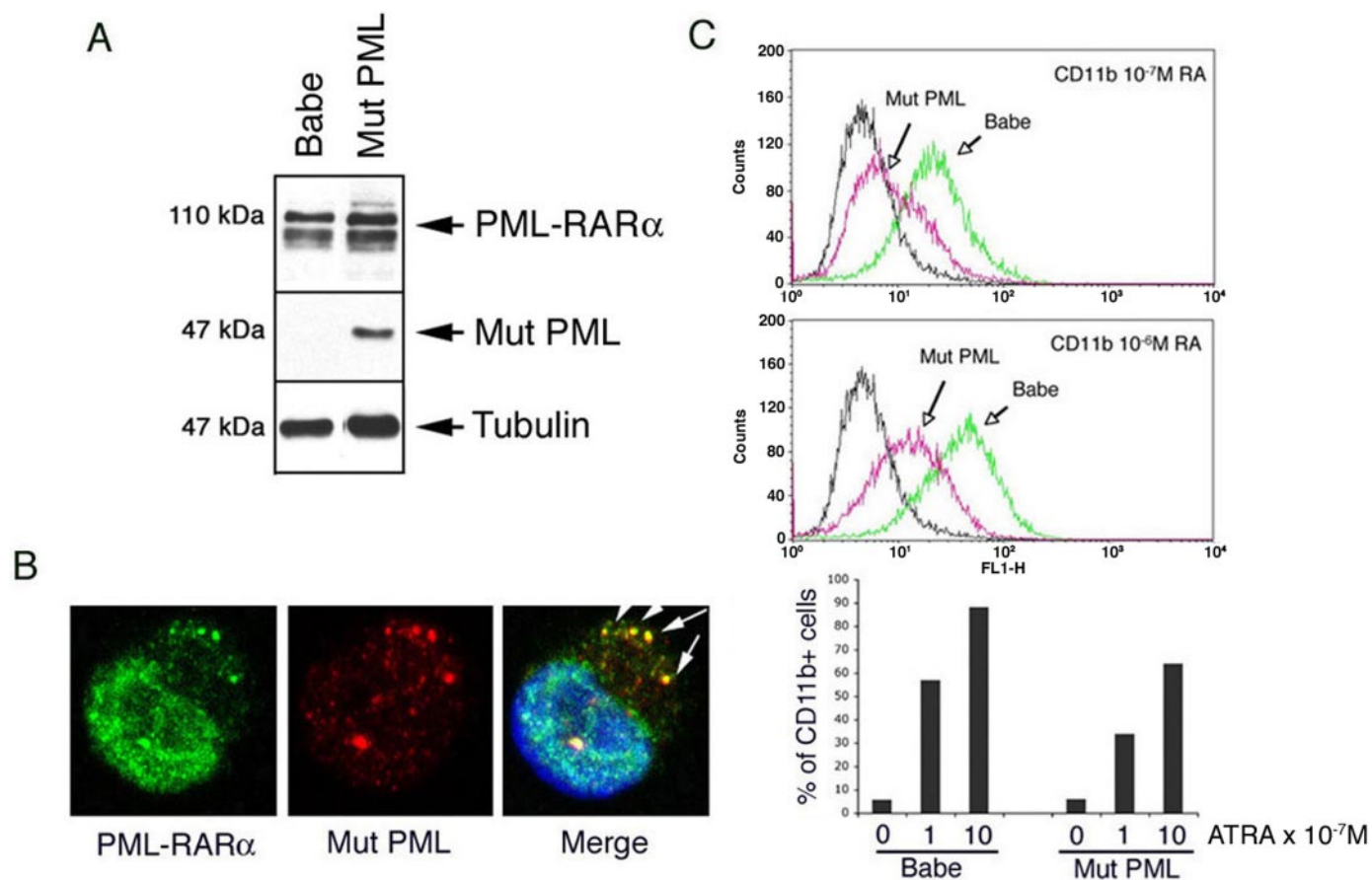


FIGURE 3. Mut PML inhibits RA-dependent differentiation in transduced NB4 cells. *A* and *B*, NB4 cells were infected with Mut PML retroviruses and analyzed for expression of PML-RAR α and Mut PML by Western blot (*A*) and immunofluorescence (*B*). *C*, Mut PML inhibits RA-induced differentiation. Differentiation was evaluated by fluorescence-activated cell sorter using an antibody directed against the granulocytic-monocytic maturation marker CD11b after 3 days of culture in the presence of either vehicle or 0.1/1.0 μM RA. The CD11b expression pattern in untreated control (Babe)- and Mut PML-infected cells was undistinguishable.

whether Mut PML could affect differentiation in the context of APL cells, we transduced the APL cell line NB4 with Mut PML and analyzed the sensitivity to ATRA (Fig. 3*A*). Mut PML and PML-RAR α partially colocalized in cytoplasmic bodies in these cells (Fig. 3*B*). Vector- and Mut PML-transduced cells were cultured in the presence of ATRA and analyzed for the expression of the differentiation marker CD11b. Remarkably, in Mut PML-transduced NB4 cells differentiation induced by pharmacological concentrations of ATRA was reduced (Fig. 3*C*). This indicates that Mut PML is able to potentiate PML-RAR α activity in the context of APL.

Cytosolic PML-RAR α Inhibits the Response to RA—Previous reports have shown that overexpressed PML-RAR α localizes to the cytoplasm (18, 28–30). We confirmed that in a fraction of transfected fibroblasts (~40%) PML-RAR α accumulates in cytoplasmic structures reminiscent of PML-CB (Fig. 4*D* and not shown). We then analyzed the distribution of overexpressed full-length PML-RAR α by subcellular fractionation and found that it accumulated in both nuclear and cytoplasmic fractions (Fig. 4*A*). Moreover, endogenous PML-RAR α accumulated in the cytosolic fraction of an APL cell line, NB4 (Fig. 4*B*).

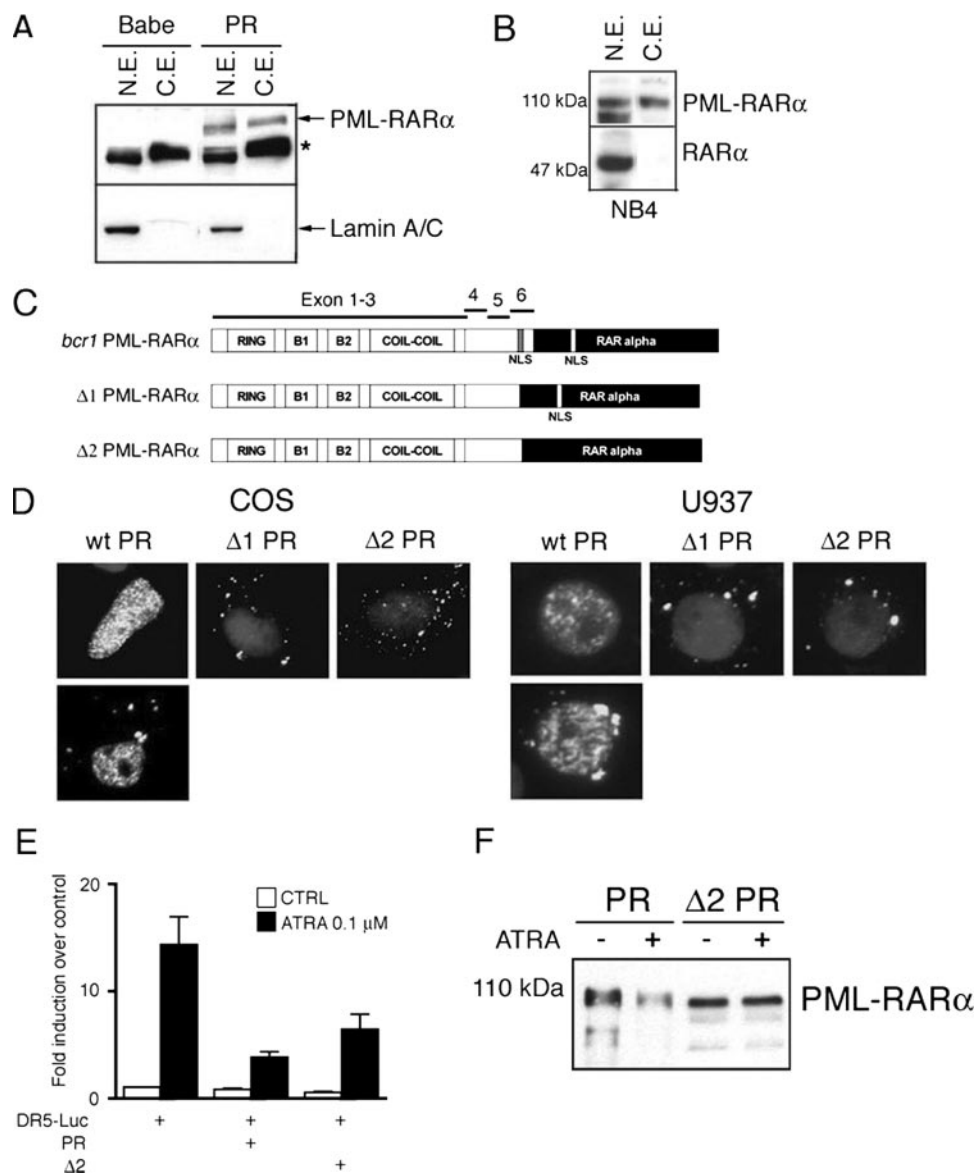
To analyze the consequences of cytoplasmic localization of PML-RAR α , we constructed *bcr1* PML-RAR α mutants lacking PML nls only ($\Delta 1$ PR) or both PML and RAR α nls ($\Delta 2$ PR) (Fig. 4*C*). $\Delta 1$ and $\Delta 2$ PR mutants were expressed in both COS1 and U937 cells (Fig. 4*D*). Immunofluorescence analyses demonstrated that although wild type PML-RAR α was found either in the nucleus only (60% cells; Fig. 4*D*, upper panel) or in both the nucleus and the cytoplasm (40% cells; Fig. 4*D*, lower panel), $\Delta 2$ PR was

instead exclusively cytoplasmic (Fig. 4*D*). Interestingly, $\Delta 1$ PR predominantly accumulated in the cytoplasm, thus suggesting that PML nls governs the nuclear localization of PML-RAR α (Fig. 4*D*). We then studied the transcriptional properties of the PR mutants in COS1 cells. Surprisingly, we found that both $\Delta 2$ and $\Delta 1$ PR are fully capable of inhibiting ATRA-dependent transcription (Fig. 4*E* and not shown). Furthermore, we observed that $\Delta 2$ PR is not down-regulated upon RA treatment, thus suggesting that cytoplasmic localization of PML-RAR α results in its impaired degradation (Fig. 4*F*).

Based on these findings, we conjectured that cytoplasmic PML-RAR α could induce the delocalization of essential transcriptional regulators to the cytoplasm. Previous reports have shown that PML-RAR α induces the delocalization of the RA receptor component RXR α to aberrant nuclear and cytoplasmic foci (29). Remarkably, we also found that $\Delta 2$ PR causes the relocation of both endogenous and exogenous RXR α to PML-CB (Fig. 5*A* and data not shown). To determine whether delocalization of RXR α is required for transcriptional inhibition, we constructed a $\Delta 2$ PR mutated at residues essential for RXR α binding ($\Delta 2$ M883R/T886R) (21). $\Delta 2$ M883R/T886R was less potent in repressing ATRA-dependent transcription, indicating that RXR α recruitment is required at least in part for transcriptional repression (Fig. 5*B*). We next tested whether vitamin D₃ (VD₃)-dependent transcription, which relies on RXR α and is repressed by WT PML-RAR α , was inhibited by $\Delta 2$ PR (Fig. 5*C*). Indeed, endogenous VD₃ receptor activity is repressed by cytoplasmic PR to an extent similar to WT PR (Fig. 5*C*).

Mut PML and PML-RAR α Have Cytoplasmic Functions

FIGURE 4. Cytoplasmic PML-RAR α inhibits ATRA-dependent transcription and differentiation. *A*, overexpressed PML-RAR α accumulates in nuclear (N.E) and cytosolic (C.E) extracts. Nuclear and cytosolic extracts from control (*Babe*) and *bcr1* PML-RAR α (PR)-infected cells were probed with anti-RAR α antibody. Lamin A/C was detected as control of purity of the cytoplasmic fraction. *B*, PML-RAR α accumulates in cytoplasmic fractions of APL cells. APL fractions were analyzed for the presence of RAR α and PML-RAR α using anti-RAR α antibody. RAR α is shown as control for nuclear fractions, as lamin A/C is not detectable in NB4 cells. *C*, scheme of *bcr1* PML-RAR α and nls mutants. *D*, deletion of PML-RAR α nls results in localization to PML-CB. COS1 (left panel) and U937 cells (right panel) were transfected with PML-RAR α mutants lacking either PML ($\Delta 1$ PR) or both PML and RAR α ($\Delta 2$ PR) nls. Cells were stained with anti-RAR α antibodies and counterstained with DAPI and analyzed by immunofluorescence and confocal microscopy. *E*, $\Delta 2$ PR ($\Delta 2$) inhibits ATRA-dependent transcription. A DR5-luciferase reporter (DR5-Luc) was transfected into COS1 cells alone or in combination with wild type (wt) PML-RAR α (PR) and $\Delta 2$ mutants, in the presence or absence of 0.1 μ M ATRA. *F*, $\Delta 2$ PR is not down-regulated upon ATRA treatment. Transfected COS1 cells were cultured in the absence or presence of 0.1 μ M ATRA and analyzed for WT (PR) and $\Delta 2$ PR expression using an anti-RAR α antibody. Extracts were normalized by β -galactosidase staining.



Cytosolic PML-RAR α Inhibits Differentiation of Hematopoietic Cells—To determine whether $\Delta 2$ PR-mediated impairment of RA-dependent transcription has functional consequences on the maturation of hematopoietic cells, we transduced U937 cells with $\Delta 2$ PR retroviruses and analyzed the sensitivity of the resulting clones to ATRA-induced differentiation (Fig. 6A). Strikingly, the morphology of ATRA-treated $\Delta 2$ PR-expressing cells was almost indistinguishable from control cells, and many mitotic figures were readily detectable in ATRA-treated $\Delta 2$ PR cells (Fig. 6B). Accordingly, the expression of the maturation marker CD11b upon ATRA treatment was inhibited in $\Delta 2$ PR-transduced U937 clones (Fig. 6C).

***bcr3* PML-RAR α Largely Localizes to the Cytoplasm and Colocalizes with RXR α —**We next analyzed the localization pattern of the *bcr3* PML-RAR α form (Fig. 7A), which lacks the PML nls (2, 3), and found, remarkably, that it was predominantly cytoplasmic (Fig. 7, A and B). Moreover, as for $\Delta 2$ PR, *bcr3* PML-RAR α colocalized with both overexpressed and endogenous RXR α (Fig. 7, A and B). Finally, we analyzed the subcellular distribution of PML-RAR α in primary APL cells carrying the *bcr3* breakpoint and found that a substantial amount of PML-RAR α accumulates in the cytoplasm (Fig. 7C). Furthermore, RXR α predomi-

nantly partitioned to the cytoplasmic fractions, thus indicating that cytoplasmic PML-RAR α also induces RXR α delocalization in primary APL cells (Fig. 7C).

DISCUSSION

PML-RAR α -mediated leukemogenesis is believed to occur mainly through chromatin remodeling, which leads to dramatic changes in the transcriptome of hematopoietic cells. However, limited information is available about the mechanisms that could promote transformation without a direct effect on chromatin. Our work indicates that cytosolic localization of PML and PML-RAR α can affect transcription and promote a differentiation block in hematopoietic cells.

Cytosolic PML Mutants Accumulate in Doughnut-shaped Cytoplasmic Bodies—We have demonstrated that Mut PML forms novel cytoplasmic structures, which we named PML-CB, and closely resembles the PML-NB in EM analyses. This suggests that essential components of the two structures could be shared. Alternatively, PML could be the core and essential component required for the assembly of the doughnut-shaped body. The fact that Mut PML associates with the insoluble part of the cytoplasm originally prompted us to investigate

FIGURE 5. RXR α is delocalized to PML-CB by cytoplasmic PML-RAR α . *A*, cytoplasmic PML-RAR α causes RXR α relocation to PML-CB. After transfection with $\Delta 2$ PR, COS1 cells were stained with anti-HA and RXR α antibodies and counterstained with DAPI. *B*, $\Delta 2$ PR mutant impaired in RXR α binding ($\Delta 2$ M883R/T886R) is less potent in inhibiting ATRA-dependent transcription. Cells were transfected and treated as mentioned above. *C*, $\Delta 2$ PR inhibits vitamin D₃ (VD₃)-induced transcription. A VD₃-luciferase reporter (*VDR-Luc*) was transfected into COS1 cells alone or in combination with wild type PML-RAR α (PR) and $\Delta 2$ mutant in the presence or absence of 1 μ M VD₃.

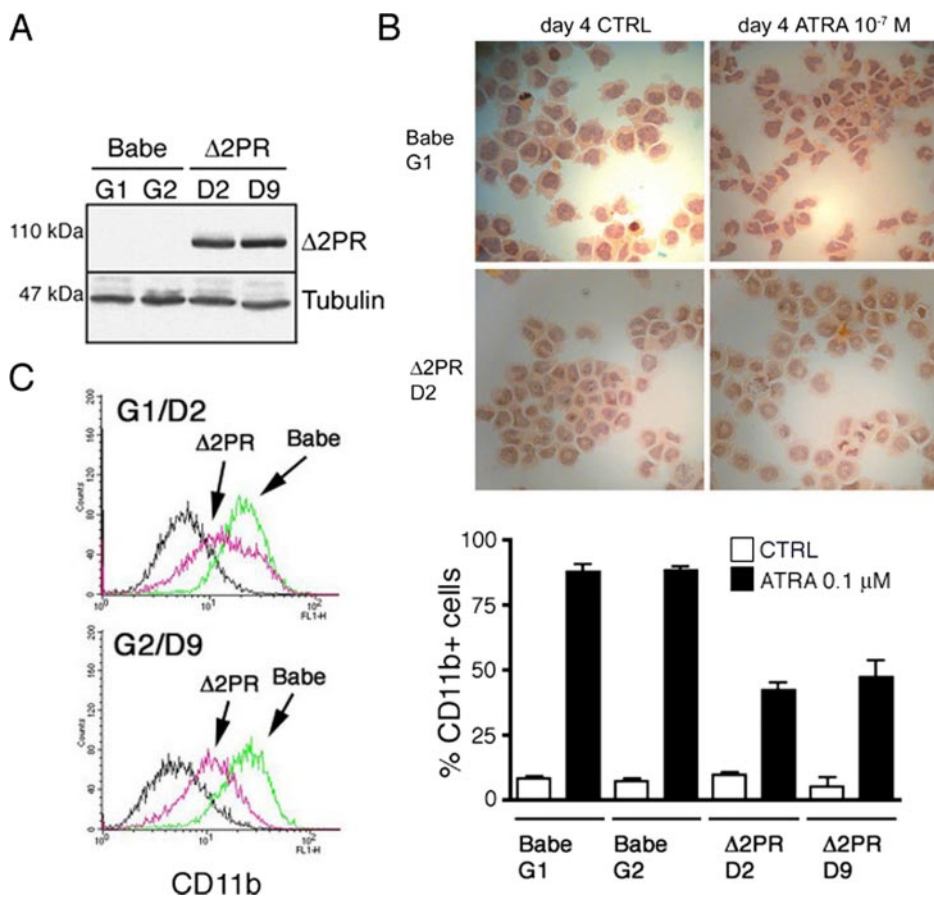
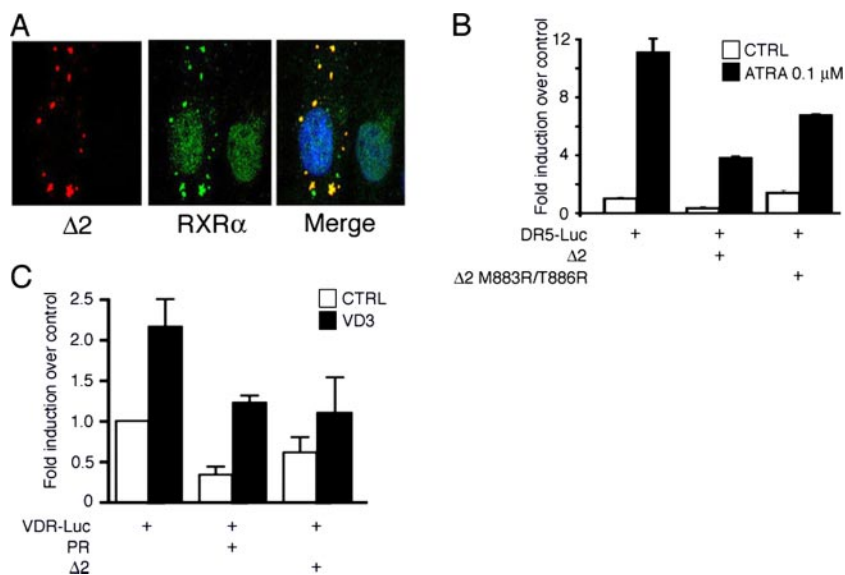


FIGURE 6. Cytoplasmic PML-RAR α inhibits RA-induced differentiation. *A*, expression levels of $\Delta 2$ PR in infected U937 clones were analyzed using an anti-RAR α antibody. *B*, morphological changes in control (*G1*) and $\Delta 2$ PR (*D2*)-expressing cells. Cells cultured with 10^{-7} M ATRA for 4 days were cytopun and stained with hematoxylin-eosin. *C*, $\Delta 2$ PR inhibits ATRA-dependent differentiation in transduced U937 cells. $\Delta 2$ PR-expressing (*D2* and *D9*) and control (*G1* and *G2*) clones were treated with 0.1 μ M RA and analyzed for CD11b expression by fluorescence-activated cell sorter at day 3. Intensity of CD11b staining and percentage of CD11b+ cells are shown (*left* and *right* panels, respectively). CD11b expression levels in untreated control (*G1* and *G2*)- and $\Delta 2$ PR-infected cells (*D2* and *D9*) were undistinguishable.

whether it could colocalize with cytoplasmic organelles. However, we were unable to demonstrate any colocalization with known organelles. In particular, Mut PML does not associate with endosomes, as it is known for a cytoplasmic PML isoform (13). It is therefore possible that the association with endosomes may be lost in APL cells expressing truncated PML mutants. While analyzing the distribution of various PML-NB components, we found that CBP relocates to PML-CB in Mut PML-expressing cells, whereas Daxx and Sp100 do not. It is reasonable

to hypothesize that CBP redistribution could have functional consequences on the activation of selected transcription factors.

Mut PML Potentiates PML-RAR α —We found that Mut PML colocalizes and interacts with PML-RAR α in both adherent cells and leukemic blasts. Surprisingly, Mut PML potentiates PML-RAR α -mediated repression of RA-dependent transcription, thus suggesting that cytoplasmic localization of PML-RAR α may result in transcriptional inhibition in the absence of direct effects on chromatin. Remarkably, expres-

Mut PML and PML-RAR α Have Cytoplasmic Functions

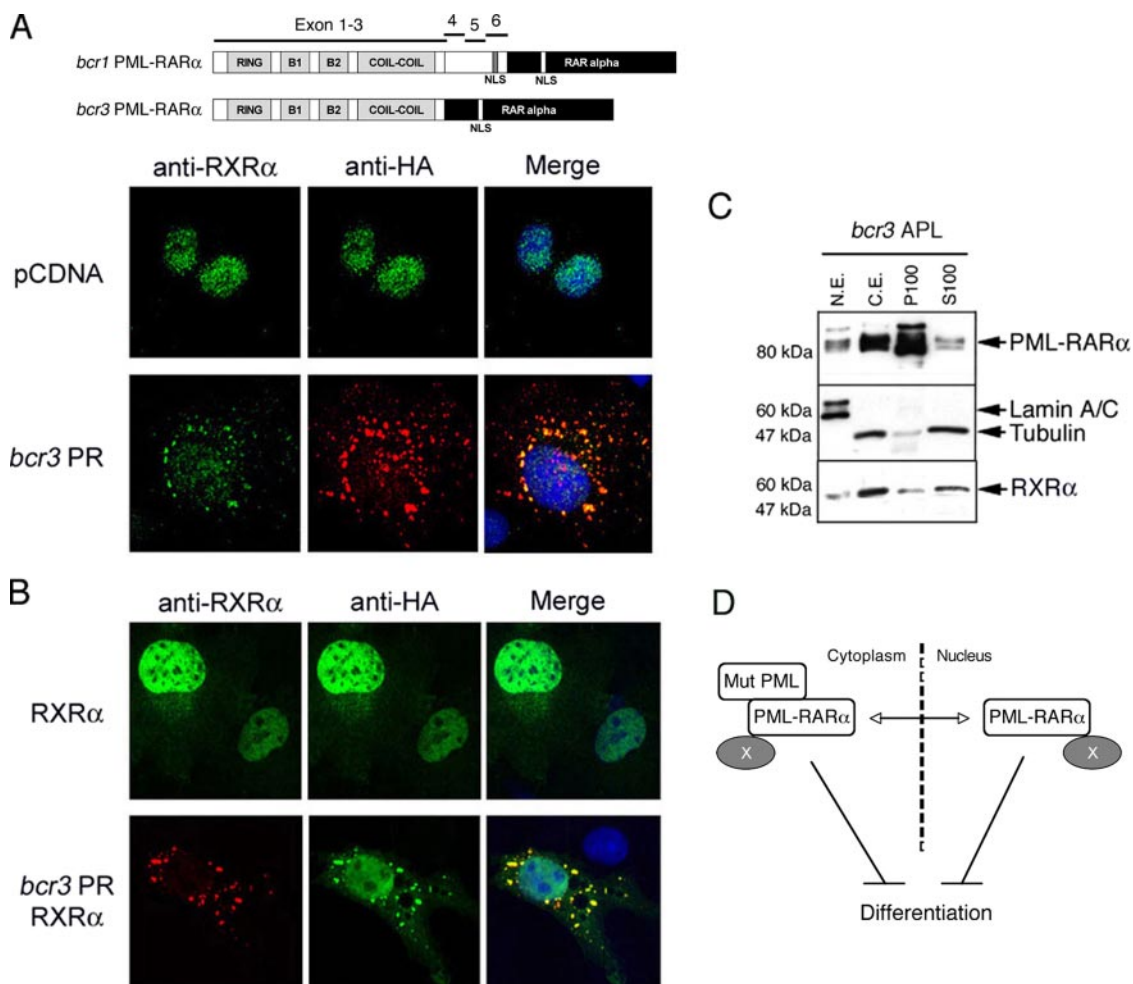


FIGURE 7. *bcr3* PML-RAR α accumulates in the cytoplasm and delocalizes RXR α . *A*, *bcr3* PML-RAR α is predominantly cytoplasmic and colocalizes with endogenous RXR α . The upper panel shows a schematic representation of Bcr1 and Bcr3 proteins. Lower panels, HA-*bcr3* PML-RAR α -transfected COS1 cells were probed with an anti-HA antibody, counterstained with DAPI, and analyzed by confocal microscopy. *B*, overexpressed RXR α colocalizes with *bcr3* PML-RAR α in the cytoplasm. HA-*bcr3* PML-RAR α /RXR α - and RXR α -transfected COS1 cells were probed with anti-HA and anti-RXR α antibodies, counterstained with DAPI, and analyzed by confocal microscopy. *C*, *bcr3* PML-RAR α and RXR α accumulate in the cytosolic fraction of primary APL cells. APL cells from a patient carrying the *bcr3* translocation were fractionated into nuclear extracts (N.E.) and cytosolic fractions (total cytoplasmic extracts (C.E.), pellet, P100; supernatant, S100). Filters were probed with anti-RAR α , RXR α , lamin A/C, and tubulin antibodies. *D*, working model. Cytoplasmic localization of PML-RAR α , alone or through binding to Mut PML, does not affect its ability to repress differentiation. Delocalization of components of the RA receptor complex (X), such as RXR α , is one of the potential mechanisms involved.

sion of Mut PML in APL cells counteracts differentiation induced by pharmacological doses of RA. Furthermore, we demonstrated that Mut PML hampers PML-RAR α degradation induced by RA, thus providing a mechanistic explanation for the observed resistance to RA. It is possible that Mut PML can interfere with the proteasome-mediated degradation of PML-RAR α , which is as yet poorly characterized. Another possibility is that Mut PML modulates PML-RAR α SUMOylation, which has been shown to be essential for PML-RAR α -transforming capacity (21).

Cytosolic PML-RAR α Inhibits Transcription and Differentiation—Consistent with previous reports (18, 28–30), we found that overexpressed PML-RAR α can locate to the cytoplasm. In addition, we demonstrated that endogenous PML-RAR α accumulates in the cytoplasmic fraction of APL cells, thus suggesting it can bear cytoplasmic functions. To test this, we analyzed whether a PML-RAR α mutant ($\Delta 2$ PR) that localizes to the cytoplasm retains the ability of inhibiting RA-dependent transcription. Indeed, $\Delta 2$ PR is almost as potent as WT PML-RAR α in repressing RA-triggered transcription. $\Delta 2$ PR is not down-regulated upon RA, thus again supporting the hypothesis that cytoplasmic localization of PML-RAR α inhibits its RA-dependent degradation. Interestingly, $\Delta 2$ PR colocalizes with RXR α in PML-CB. It is of note that the

cytoplasmic redistribution of RXR α has been reported to cause an impairment in its transcriptional function (31). We have found that mutations abolishing RXR α binding substantially reduce $\Delta 2$ PR repressing activity, thus suggesting that RXR α relocation is one of the potential mechanisms involved. As the rescue is not complete, it is conceivable that other mechanisms may contribute to the observed phenomena. $\Delta 2$ PR appears to be a potent inhibitor of differentiation as it represses differentiation in U937 cells at pharmacological doses of RA. Interestingly, we found that although $\Delta 2$ PR causes a 50% reduction of CD11b $^{+}$ cells compared with ATRA treatment, the morphology of RA-treated $\Delta 2$ PR-infected cells is nearly undistinguishable from untreated cells. Moreover, proliferation is not substantially blocked in $\Delta 2$ PR-expressing cells, which continue to proliferate even at high concentrations of ATRA (1 μ M).³ This aspect warrants further investigation in the near future. Finally, we found that the *bcr3* form of PML-RAR α , which has been associated with poor prognosis in a number of studies (2, 3), localizes to the cytoplasm at a greater extent than the *bcr1* form and causes the redistribution of RXR α to PML-CB. In cells from an APL patient

³ C. Bellodi and P. Salomoni, unpublished observations.

carrying the *bcr3* break point, a large fraction of PML-RAR α is found in the cytosol, where also RXR α accumulates. Overall, our findings suggest that PML-RAR α cytoplasmic pool may affect transcription and differentiation in the absence of direct effects on chromatin-dependent phenomena (Fig. 7D).

Acknowledgments—We thank Saverio Minucci (IEO, Milan, Italy), Carlo Gambacorti (Istituto Tumori, Milan, Italy), Martin Dyer, Renata Walewska, Karen Pinkoski, Michael Pinkoski (MRC, Leicester, UK), Keith Leppard (Warwick University, UK), Thomas Hofmann, Hans Will (Heinrich-Pette-Institute, Hamburg, Germany), Bruno Calabretta (Thomas Jefferson University, Kimmel Cancer Center, Philadelphia), and Karsten Carlberg (University of Kuopio, Finland) for reagents, protocols, and useful discussions. We also thank Kulvinder Sikand for confocal microscopy analysis and Tim Smith and Judy McWilliam for EM studies (MRC, Toxicology Unit, Leicester, UK).

REFERENCES

- Salomoni, P., and Pandolfi, P. P. (2002) *Cell* **108**, 165–170
- Huang, W., Sun, G. L., Li, X. S., Cao, Q., Lu, Y., Jang, G. S., Zhang, F. Q., Chai, J. R., Wang, Z. Y., and Waxman, S. (1993) *Blood* **82**, 1264–1269
- Vahdat, L., Maslak, P., Miller, W. H., Jr., Eardley, A., Heller, G., Scheinberg, D. A., and Warrell, R. P., Jr. (1994) *Blood* **84**, 3843–3849
- Grignani, F., Ferrucci, P. F., Testa, U., Talamo, G., Fagioli, M., Alcalay, M., Mencarelli, A., Peschle, C., Nicoletti, I., and Pelicci, P. G. (1993) *Cell* **74**, 423–431
- Grignani, F., De Matteis, S., Nervi, C., Tomassoni, L., Gelmetti, V., Cioce, M., Fanelli, M., Ruthardt, M., Ferrara, F. F., Zamir, I., Seiser, C., Lazar, M. A., Minucci, S., and Pelicci, P. G. (1998) *Nature* **391**, 815–818
- Lin, R. J., Nagy, L., Inoue, S., Shao, W., Miller, W. H., Jr., and Evans, R. M. (1998) *Nature* **391**, 811–814
- Di Croce, L., Raker, V. A., Corsaro, M., Fazi, F., Fanelli, M., Faretta, M., Fuks, F., Lo Coco, F., Kouzarides, T., Nervi, C., Minucci, S., and Pelicci, P. G. (2002) *Science* **295**, 1079–1082
- Zhu, J., Lallemand-Breitenbach, V., and de The, H. (2001) *Oncogene* **20**, 7257–7265
- Chen, G. Q., Shi, X. G., Tang, W., Xiong, S. M., Zhu, J., Cai, X., Han, Z. G., Ni, J. H., Shi, G. Y., Jia, P. M., Liu, M. M., He, K. L., Niu, C., Ma, J., Zhang, P., Zhang, T. D., Paul, P., Naoe, T., Kitamura, K., Miller, W., Waxman, S., Wang, Z. Y., de The, H., Chen, S. J., and Chen, Z. (1997) *Blood* **89**, 3345–3353
- Zhu, J., Koken, M. H., Quignon, F., Chelbi-Alix, M. K., Degos, L., Wang, Z. Y., Chen, Z., and de The, H. (1997) *Proc. Natl. Acad. Sci. U. S. A.* **94**, 3978–3983
- Rego, E. M., Wang, Z. G., Peruzzi, D., He, L. Z., Cordon-Cardo, C., and Pandolfi, P. P. (2001) *J. Exp. Med.* **193**, 521–529
- Jensen, K., Shiels, C., and Freemont, P. S. (2001) *Oncogene* **20**, 7223–7233
- Lin, H. K., Bergmann, S., and Pandolfi, P. P. (2004) *Nature* **431**, 205–211
- Gurrieri, C., Nafa, K., Merghoub, T., Bernardi, R., Capodice, P., Biondi, A., Nimer, S., Douer, D., Cordon-Cardo, C., Gallagher, R., and Pandolfi, P. P. (2004) *Blood* **103**, 2358–2362
- Zheng, P., Guo, Y., Niu, Q., Levy, D. E., Dyck, J. A., Lu, S., Sheiman, L. A., and Liu, Y. (1998) *Nature* **396**, 373–376
- Pandolfi, P. P., Alcalay, M., Fagioli, M., Zangrilli, D., Mencarelli, A., Diverio, D., Biondi, A., Lo Coco, F., Rambaldi, A., and Grignani, F. (1992) *EMBO J.* **11**, 1397–1407
- Alcalay, M., Zangrilli, D., Fagioli, M., Pandolfi, P. P., Mencarelli, A., Lo Coco, F., Biondi, A., Grignani, F., and Pelicci, P. G. (1992) *Proc. Natl. Acad. Sci. U. S. A.* **89**, 4840–4844
- Khan, M. M., Nomura, T., Chiba, T., Tanaka, K., Yoshida, H., Mori, K., and Ishii, S. (2004) *J. Biol. Chem.* **279**, 11814–11824
- Lane, A. A., and Ley, T. J. (2003) *Cell* **115**, 305–318
- Morgenstern, J. P., and Land, H. (1990) *Nucleic Acids Res.* **18**, 1068
- Zhu, J., Zhou, J., Peres, L., Riaucoux, F., Honore, N., Kogan, S., and de The, H. (2005) *Cancer Cell* **7**, 143–153
- Haze, K., Yoshida, H., Yanagi, H., Yura, T., and Mori, K. (1999) *Mol. Biol. Cell* **10**, 3787–3799
- Salomoni, P., Bernardi, R., Bergmann, S., Changou, A., Tuttle, S., and Pandolfi, P. P. (2005) *Blood* **105**, 3686–3690
- Hofmann, H., Sindre, H., and Stamminger, T. (2002) *J. Virol.* **76**, 5769–5783
- Khelifi, A. F., D'Alcontres, M. S., and Salomoni, P. (2005) *Cell Death Differ.* **12**, 5471–5476
- Dinsdale, D., Green, J. A., Manson, M. M., and Lee, M. J. (1992) *Histochem. J.* **24**, 144–152
- Lin, R. J., and Evans, R. M. (2000) *Mol. Cell* **5**, 821–830
- Kastner, P., Perez, A., Lutz, Y., Rochette-Egly, C., Gaub, M. P., Durand, B., Lanotte, M., Berger, R., and Chambon, P. (1992) *EMBO J.* **11**, 629–642
- Perez, A., Kastner, P., Sethi, S., Lutz, Y., Reibel, C., and Chambon, P. (1993) *EMBO J.* **12**, 3171–3182
- Koken, M. H., Puvion-Dutilleul, F., Guillemain, M. C., Viron, A., Linares-Cruz, G., Stuurman, N., de Jong, L., Szostecki, C., Calvo, F., Chomienne, C., Degos, L., Puvion, E., and de Thé, H. (1994) *EMBO J.* **13**, 1073–1083
- Katagiri, Y., Takeda, K., Yu, Z. X., Ferrans, V. J., Ozato, K., and Guroff, G. (2000) *Nat. Cell Biol.* **2**, 435–440